LETTER

Single Image Dehazing Based on Sky Area Segmentation and Image Fusion

Xiangyang CHEN[†], **Haiyue LI**[††], **Chuan LI**[†††], *Nonmembers*, **Weiwei JIANG**[††††], *Member*, *and* **Hao ZHOU**[††,†††,†††††a)], *Nonmember*

SUMMARY Since the dark channel prior (DCP)-based dehazing method is ineffective in the sky area and will cause the problem of too dark and color distortion of the image, we propose a novel dehazing method based on sky area segmentation and image fusion. We first segment the image according to the characteristics of the sky area and non-sky area of the image, then estimate the atmospheric light and transmission map according to the DCP and correct them, and then fuse the original image after the contrast adaptive histogram equalization to improve the details information of the image. Experiments illustrate that our method performs well in dehazing and can reduce image distortion.

key words: *image dehazing, histogram equalization, image fusion, dark channel prior*

1. Introduction

Images are used more and more widely in many fields such as urban management, military defense, and industrial production, and have gradually become the main means for people to obtain information. The quality of the image directly affects the subsequent image processing effect. Images acquired in hazy weather will be seriously degraded due to atmospheric scattering, which not only affects the post-processing of images but also affects the work of various systems, such as military photoelectric reconnaissance systems. Therefore, it is important to eliminate the influence of haze on imaging.

The traditional hazy image enhancement method applies the image enhancement method to clear the image, directly improves the contrast of the image, and highlights the details, but it will cause the loss of part of the information, such as homogeneous filtering [1], histogram equalization [2] and Retinex [3], [4], etc. But this method does not achieve physical dehazing. The other is the physical model, which studies and models the causes of image degradation caused by haze, and uses the physical model to restore the hazy image. Among them, the atmospheric scattering model (ASM) [5]–[7] has attracted the attention of many scholars. Many well-known prior knowledge is used to estimate the parameters in ASM to restore the clear image, such as DCP [8], Color Attenuation Prior [9], NonLocal prior [10], etc. However, these priors are not suitable for all hazy situations and may cause unwanted artifacts. Learning-based dehazing methods have been gradually proposed in recent years, such as DehazeNet [11], AODNet [12], MSCNN [13], D^4 [14]. However, these methods require paired synthetic hazy images for training, which is prone to overfitting, and the effect on real outdoor hazy images is mediocre.

Therefore, we propose a dehazing method based on sky area segmentation and image fusion. Our contributions are summarized as follows:

- We improved the DCP, including the atmospheric light estimation and corrections to the transmission map.
- We fuse the DCP-based method with the image enhancement-based method to obtain more visually pleasing results. This fusion method can maintain the original detail information while achieving dehazing and reducing distortion.

2. Related Work

In computer vision, ASM is used to represent the imaging model of images collected in hazy scenes:

$$I(q) = J(q)t(q) + A(1 - t(q)), \tag{1}$$

where q represents the pixel coordinates, $I(q)$ denotes the hazy input, $J(q)$ represents the hazy-free output, A represents atmospheric light, $t(q)$ represents the transmission map, which describes the proportion of light reaching the camera. Image dehazing using ASM is to estimate A and $t(q)$ to solve for $J(q)$:

$$J(q) = \frac{I(q) - A}{t(q)} + A, \tag{2}$$

DCP [8] was proposed to estimate $t(q)$, whose mathematical expression is:

Manuscript received February 8, 2023.
Manuscript revised March 27, 2023.
Manuscript publicized April 24, 2023.

[†]The author is with School of General Courses, Anqing Medical College, AnQing 246052, Anhui, China.
[††]The authors are with School of Big Data and Artificial Intelligence, Chizhou University, Chizhou 247100, Anhui, China.
[†††]The authors are with College of Big Data and Intelligent Engineering, Chongqing College of International Business and Economics, Chongqing 401520, China.
[††††]The author is with School of Information and Communication Engineering, Beijing University of Posts and Telecommunications, Beijing 100876, Beijing, China.
[†††††]The author is with Anhui Engineering Laboratory for Intelligent Applications and Security of Industrial Internet, Anhui University of Technology, Ma'anshan, Anhui, 243032, China.
a) E-mail: zhouhao19@email.swu.edu.cn (Corresponding author)

DOI: 10.1587/transinf.2023EDL8010

$$J^{dark}(q) = \min_{y\in\Omega(q)} (\min_{c\in\{r,g,b\}} J^c(y)), \tag{3}$$

where $J^{dark}(q)$ represents the dark channel map of $J(q)$, $\Omega(q)$ denotes a patch centered at pixel q. DCP finds that $J^{dark}(q)$ is close to 0 through the statistics of images, then $t(q)$ can be estimated as:

$$t(q) = 1 - \omega^* \min_{y\in\Omega(q)} \left(\min_{c\in\{r,g,b\}} \frac{I^c(y)}{A^c} \right), \tag{4}$$

where ω is to keep distant objects more haze, and it is set to 0.95 in DCP [8]. DCP also introduces the estimation method of A. Take the brightest 0.1 percent pixel from the dark channel of $I(q)$, and then find the value of the pixel with the highest intensity value in $I(q)$ as the estimated value of A. Then $J(q)$ can be recovered by Eq. (2). DCP-based methods [22] have received a lot of attention due to its simplicity and effectiveness. However, DCP will fail in the sky area, which will generate noise and affect the visual effect. Different from the literature [22], we adopted a new segmentation method based on the characteristics of the sky region, proposed a new method for estimating atmospheric light and correcting transmission, and combined image enhancement methods to fuse multiple enhanced images to improve the quality of human visual perception.

3. Proposed Method

The process of dehazing is to estimate parameters A and $t(q)$, and then solve $J(q)$ according to ASM (Eq. (1)). We first segment the image to be processed into the sky and non-sky area and then estimate A separately for fusion. Second, we correct the $t(q)$ estimated by the DCP to obtain a more accurate $t(q)$. Third, we solve for $J(q)$ according to ASM. Finally, we enhance $J(q)$ through image fusion to obtain high-quality images that can better meet the human vision.

3.1 Image Segmentation

Traditional methods based on sky region segmentation mainly utilized histogram analysis, artificial thresholding, or clustering methods [26]–[28]. Although these methods could show better segmentation results in some cases, they needed to manually set the corresponding threshold parameters, or were limited to clustering operations. Hence, these methods were not universal and had the possibility of misjudgment.

To accurately segment the sky area of the image to more properly use DCP, we use the method proposed by Li [15]. Based on a large number of statistical analyses, this method proposed a new sky area feature prior, and then accurately divides the hazy image into sky region and non-sky area. This method can basically completely identify the sky area of the image, can effectively eliminate the misjudgment effect caused by highlight noise, and had a certain degree of robustness. According to this prior, the sky feature $F(q)$ is:

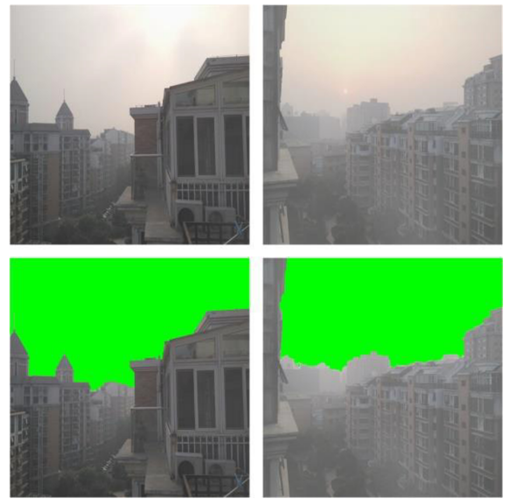

Fig. 1 Sky region segmentation results. The first row is the hazy image, and the second row is the segmentation result, where the green area represents the segmented sky area.

$$\begin{aligned} F(q) = &\exp(\max(0, (\lambda_1 - \nabla(q)))) \\ &+ \exp(\max(0, (V(q) - 1.2 * \overline{V}))) \\ &+ \exp(\max(0, (\lambda_2 - S(q)))), \end{aligned} \tag{5}$$

where q represents the pixel coordinates, $\nabla(q)$, $V(q)$ and $S(q)$ are the gradient component, brightness component and saturation component respectively, $\overline{V}$ is the average brightness value of the whole image, $\lambda_1 = 0.005$ and $\lambda_2 = 0.04$ are the feature thresholds by this prior, respectively. Furthermore, the constructed sky feature $F(q)$ is used to judge the sky area, that is, when the sky feature value $F(q)$ of a certain pixel is greater than a certain multiple of the sky feature mean value of the whole image (default 1.2 times), it is determined that the pixel is part of the sky area I_{sky}, otherwise it belongs to the non-sky area $I_{non-sky}$. If the image size is m*n, we record the number of pixels in the sky area as *numSky*. The segmentation results are shown in Fig. 1.

3.2 Estimation of A

First, we convert the input image to grayscale, then we estimate A_1 of the entire image according to the DCP, and we use the average value of the pixels in I_{sky} as A_2:

$$A_2 = \frac{S_{sky}}{numSky}, \tag{6}$$

where S_{sky} represents the sum of pixel values in I_{sky}. The ratio K of the number of pixels in I_{sky} to the total pixels of the image is:

$$K = \frac{numSky}{m * n}, \tag{7}$$

Then our estimated atmospheric light value A is:

$$A = A_1 * (1 - K) + A_2 * K, \tag{8}$$

Our estimated A combines the advantages of DCP and avoids the disadvantage of DCP failure in the sky area.

3.3 Correction of Transmission Map $t(q)$ Based on DCP Estimation

Since $t(q)$ estimated by the DCP is usually lower than the true value [9], this will cause errors and lead to noise amplification. Therefore, in order to reduce the error of $t(q)$ estimation, we adopt Wiener filtering [16] to correct $t(q)$ estimated by Eq. (4), and then we adopt guided filtering [17] to refine $t(q)$. According to our estimated A and $t(q)$, the clear $J(q)$ can be recovered via Eq. (2).

3.4 Image Fusion

Since the image restored by the DCP method will be darker and the color will be distorted, the visual perception effect of the human eye is not satisfactory. Therefore, we propose a fusion method to improve restoration quality and reduce distortion. First, we enhance the original $I(q)$ through the Constrained Adaptive Histogram Equalization Algorithm (CLAHE) [18] to obtain the effect of less haze in human vision. The CLAHE algorithm controls the enhanced contrast by setting the *clip limit* (or *contrast factor*) parameter. The larger the parameter value, the greater the contrast, and vice versa. In our dehazing task, we have found through experiments that for slightly hazy images, setting the *clip limit* to 0.001 can enhance the detail information, while for dense hazy images, setting the *clip limit* to 0.02 can not only better enhance the details but also effectively reduce the dense hazy effect.

We extract the three channels (RGB) of the original hazy image $I(q)$ as $IR(q)$, $IG(q)$ and $IB(q)$, and then use the CLAHE algorithm to enhance them respectively, and then perform mean fusion with the three channel components $JR(q)$, $JG(q)$, and $JB(q)$ of our dehazed image $J(q)$:

$$\begin{aligned} \overline{JR}(q) &= \frac{IR(q) + JR(q)}{2} \\ \overline{JG}(q) &= \frac{IG(q) + JG(q)}{2}, \\ \overline{JB}(q) &= \frac{IB(q) + JB(q)}{2} \end{aligned} \tag{9}$$

where $\overline{JR}(q)$, $\overline{JG}(q)$ and $\overline{JB}(q)$ are the three channel components after fusion, and finally we synthesize these three components into a complete image $\overline{J}(q)$, which is the final clear image of our method.

4. Experiments

4.1 Quantitative and Qualitative Experiments

We prove the performance of our method through quantitative and qualitative experiments, comparing it with state-of-the-art methods including DCP [8], Meng [19], NonLocal [10], MSCNN [13], DehazeNet [11], AODNet [12], He [20], Ehsan [21], Zhou [22], and D4 [14]. For quantitative evaluation, we adopt the widely used PSNR and SSIM [23] evaluation metrics. We randomly selected a synthetic hazy image from SOTS-Outdoor dataset (RESIDE [24]) and selected a real hazy image from NH-Haze dataset [25] for experiments. From Image1 in Fig. 2, the result recovered by DCP are darker, the result recovered by Meng, AODNet, Ehsan and D4 have poor sky area effects, the result recovered by DehazeNet and He is oversaturated,

Fig. 2 Visual comparison results with other state-of-the-art methods. Image1 is a synthetic hazy image from RESIDE dataset [24], and Image 2 is a real hazy image from NH-Haze dataset [25].

Table 1 Quantitative experimental comparison results for Fig. 2

Image	DCP	Meng	NonLocal	MSCNN	DehazeNet	AODNet	He	Ehsan	Zhou	D4	Our
	PSNR/SSIM	PSNR/SSIM	PSNR/SSIM	PSNR/SSIM	PSNR/SSIM	PSNR/SSIM	PSNR/SSIM	PSNR/SSIM	PSNR/SSIM	PSNR/SSIM	PSNR/SSIM
Image 1	11.769/0.713	17.565/0.821	19.623/0.865	21.916/0.897	16.124/0.730	15.113/0.790	22.512/0.896	13.623/0.692	22.656/0.925	18.042/0.873	**22.784/0.933**
Image 2	11.812/0.267	15.046/0.496	13.298/0.397	15.665/0.388	14.423/0.362	12.826/0.358	14.665/0.388	11.833/0.271	14.938/0.416	15.071/0.404	**15.708/0.534**

Table 2 Average quantitative comparison results of all images in SOTS-Outdoor and NH-Haze datasets

Methods	SOTS-Outdoor		NH-Haze	
	PSNR	SSIM	PSNR	SSIM
DCP	14.802	0.802	11.573	0.418
Meng	15.323	0.795	10.271	0.500
NonLocal	18.581	0.843	12.155	0.529
MSCNN	19.108	0.875	12.796	0.500
DehazeNet	18.696	0.742	11.852	0.448
AODNet	19.645	0.892	11.873	0.424
He	23.743	0.912	12.215	0.473
Ehsan	13.899	0.739	11.106	0.404
Zhou	21.970	0.900	12.419	0.515
D4	25.066	0.939	12.666	0.507
Our	**25.155**	**0.941**	**13.184**	**0.570**

and the result recovered by NonLocal and MSCNN are color distortion, while the result of our method is most similar to ground truth, and our method recovers better protection of the sky area than Zhou's method. From Image 2, various methods cannot completely remove the hazy on the dense hazy image. Other methods either have color distortion or a lot of residual haze. Our method preserves image details as much as possible while maximizing haze removal.

In addition, we perform quantitative experimental comparisons on the images in Fig. 2 and all images in the SOTS-Outdoor and NH-Haze datasets. From Table 1 and Table 2, our method has the highest indicator score, which further demonstrates the effectiveness of the method.

4.2 Ablation Study

In this section, we discuss the effectiveness of the proposed method, namely Sect. 3.2 to Sect. 3.4. We randomly selected a hazy image for the experiment, as shown in Fig. 3. We compare the original DCP method [8], and gradually add the proposed atmospheric light estimation method (i.e. Sect. 3.2), transmission map correction method (i.e. Sect. 3.3), and image fusion method (i.e. Sect. 3.4) to recover the input hazy image.

As shown in Fig. 3 (b), the sky region of the result restored by the original DCP method is severely distorted. As shown in Fig. 3 (c) that after restoration by the atmospheric light estimation method proposed in this paper, the distortion in the sky area is significantly reduced, but some areas are darker. From Fig. 3 (d), it can be seen that the result color information recovered by the proposed transmission map correction method is better. From Fig. 3 (e), it can be seen that the image fusion method proposed in this paper restores a more satisfactory visual effect, which is the closest to the ground truth image. In addition, from the PNSR/SSIM scores of each result image in Fig. 3, it can

(a) Hazy Input (b) PSNR/SSIM:15.713/0.760 (c) PSNR/SSIM:18.815/0.858
(d) PSNR/SSIM:18.909/0.865 (e) PSNR/SSIM:**26.921/0.919** (f) Ground Truth

Fig. 3 Ablation experiment visual results. (a) is the input hazy image, (b) is the result restored by the DCP method [8], (c) is the result restored by the proposed atmospheric light estimation method (that is, the method in Sect. 3.2), (d) is the result obtained by the proposed atmospheric light estimation and transmission map correction methods (i.e. the method in Sect. 3.2 and 3.3), (e) is the result restored by the proposed atmospheric light estimation, transmission map correction and image fusion method (i.e. the method in Sect. 3.2, 3.3 and 3.4).

be seen that the PNSR/SSIM scores of the images restored by the proposed methods from Sect. 3.2 to Sect. 3.4 increase sequentially. The PNSR/SSIM scores of various resulting images in Fig. 3 also demonstrate the effectiveness of each step of the proposed method.

5. Conclusions

We propose a dehazing method based on sky area segmentation and image fusion. First, the hazy image is divided into the sky area and the non-sky area, and then the atmospheric light is accurately estimated, and then the DCP estimated transmission map is corrected. Finally, we fused the original haze image enhanced by CLHE, which reduced the distortion caused by the DCP method while achieving dehazing, and restoring satisfactory results for human vision. Our method demonstrates that the fusion of prior knowledge and image enhancement methods is effective in image dehazing, which is also meaningful for the study of image restoration. In future, we will integrate more advanced prior knowledge and image enhancement methods to achieve image dehazing, making the restored result visually more satisfying.

Acknowledgments

This work was supported by the College Students' innovation and entrepreneurship training program of AnHui province (Grant No. S202211306106), the National Fund Cultivation Project of Chizhou University (CZ2021GP05), the Open Fund of Anhui Engineering Laboratory for Intelligent Applications and Security of Industrial Internet, Anhui University of Technology (IASII21-06), the Excellent Scientific Research and Innovation Team of Anhui Colleges (2022AH010098), and the Science and Technology Research Program of Chongqing Municipal Education Commission (Grant No. KJQN202102002).

References

[1] Y. Dong, L. Liu, J. Xu, and G. Wan, "Target detection algorithm based on improved homomorphic filter in haze days," 2022 Global Reliability and Prognostics and Health Management (PHM-Yantai), pp.1–5, IEEE, 2022.

[2] K. Mondal, R. Rabidas, and R. Dasgupta, "Single image haze removal using contrast limited adaptive histogram equalization based multiscale fusion technique," Multimedia Tools and Applications, pp.1–26, 2022.

[3] H. Chen, R. Chen, L. Ma, and N. Li, "Single-image dehazing via depth-guided deep retinex decomposition," The Visual Computer, pp.1–13, 2022.

[4] E.H. Land and J.J. McCann, "Lightness and retinex theory," Josa, vol.61, no.1, pp.1–11, 1971.

[5] W.E.K. Middleton, "Vision through the atmosphere," University of Toronto Press, 1952.

[6] E.J. McCartney, "Optics of the atmosphere: Scattering by molecules and particles," New York, 1976.

[7] S.G. Narasimhan and S.K. Nayar, "Vision and the atmosphere," International journal of computer vision, vol.48, no.3, pp.233–254, 2002.

[8] K.M. He, J. Sun, and X.O. Tang, "Single image haze removal using dark channel prior," IEEE Trans. Pattern Anal. Mach. Intell., vol.33, no.12, pp.2341–2353, Dec. 2011.

[9] Q. Zhu, J. Mai, and L. Shao, "A fast single image haze removal algorithm using color attenuation prior," IEEE transactions on image processing, vol.24, no.11, pp.3522–3533, 2015.

[10] D. Berman, T. Treibitz, and S. Avidan, "Non-local image dehazing," IEEE Conf. Comput. Vis. Pattern Recognit, pp.1674–1682, IEEE Computer Society, Las Vegas, NV, United states, 2016.

[11] B. Cai, X. Xu, K. Jia, C. Qing, and D. Tao, "Dehazenet: An end-to-end system for single image haze removal," IEEE Trans. Image Process., vol.25, no.11, pp.5187–5198, 2016.

[12] B. Li, X. Peng, Z. Wang, J. Xu, and D. Feng, "Aod-net: All-in-one dehazing network," IEEE Int Conf. Comput. Vision., pp.4780–4788, Institute of Electrical and Electronics Engineers Inc., Venice, Italy, 2017.

[13] W. Ren, S. Liu, H. Zhang, J. Pan, X. Cao, and M.-H. Yang, "Single image dehazing via multi-scale convolutional neural networks," European conference on computer vision, vol.9906, pp.154–169, Springer, 2016.

[14] Y. Yang, C. Wang, R. Liu, L. Zhang, X. Guo, and D. Tao, "Self-augmented unpaired image dehazing via density and depth decomposition," Proceedings of the IEEE/CVF Conference on Computer Vision and Pattern Recognition, pp.2037–2046, 2022.

[15] Y. Li, Y. Du, and Z. Gu, "Single image dehazing method via sky area recognition," Computer Engineering and Applications, vol.54, no.19, pp.204–215, 2018.

[16] B.R. Manju and M.R. Sneha, "ECG denoising using wiener filter and kalman filter,' Procedia Computer Science, vol.171, pp.273–281, 2020.

[17] K. He, J. Sun, and X. Tang, "Guided image filtering," IEEE Trans. Pattern Anal. Mach. Intell., vol.35, no.6, pp.1397–1409, June 2013.

[18] J. Ma, X. Fan, S.X. Yang, X. Zhang, and X. Zhu, "Contrast limited adaptive histogram equalization-based fusion in yiq and hsi color spaces for underwater image enhancement," International Journal of Pattern Recognition and Artificial Intelligence, vol.32, no.07, p.1854018, 2018.

[19] G. Meng, Y. Wang, J. Duan, S. Xiang, and C. Pan, "Efficient image dehazing with boundary constraint and contextual regularization," Proceedings of the IEEE international conference on computer vision (ICCV), pp.617–624, CA:IEEE, 2013.

[20] J. He, F.Z. Xing, R. Yang, and C. Zhang, "Fast single image dehazing via multilevel wavelet transform based optimization," arXiv preprint arXiv:1904.08573, 2019.

[21] S.M. Ehsan, M. Imran, A. Ullah, and E. Elbasi, "A single image dehazing technique using the dual transmission maps strategy and gradient-domain guided image filtering," IEEE Access, vol.9, pp.89055–89063, 2021.

[22] H. Zhou, Z.Z. Zhang, Y. Liu, M.Y. Xuan, W.W. Jiang, and H.L. Xiong, "Single image dehazing algorithm based on modified dark channel prior," IEICE Transactions on Information and Systems, vol.E104-D, no.10, pp.1758–1761, Oct. 2021.

[23] Z. Wang, A.C. Bovik, H.R. Sheikh, and E.P. Simoncelli, "Image quality assessment: From error visibility to structural similarity," IEEE transactions on image processing, vol.13, no.4, pp.600–612, 2004.

[24] B. Li, W. Ren, D. Fu, D. Tao, D. Feng, W. Zeng, and Z. Wang, "Reside: A benchmark for single image dehazing," IEEE Transactions on Image Processing, vol.28, pp.492–505, 2017.

[25] C.O. Ancuti, C. Ancuti, and R. Timofte, "NH-HAZE: An image dehazing benchmark with non-homogeneous hazy and haze-free images," Proceedings of the IEEE/CVF conference on computer vision and pattern recognition workshops, pp.1798–1805, 2020.

[26] G. Wang, G. Ren, L. Jiang, and T. Quan, "Single image dehazing algorithm based on sky region segmentation," Information Technology Journal, vol.12, no.6, pp.1168–1175, 2013.

[27] Y.-b. Zhu, J.-m. Liu, and Y.-g. Hao "An single image dehazing algorithm using sky detection and segmentation," 2014 7th International Congress on Image and Signal Processing (ICISP), pp.248–252, IEEE, 2014.

[28] W. Wang, X. Yuan, X. Wu, and Y. Liu, "Dehazing for images with large sky region," Neurocomputing, vol.238, pp.365–376, 2017.